Electric and Magnetic Phenomena Studied by *In Situ* Transmission Electron Microscopy

John Cumings, Eva Olsson, Amanda K. Petford-Long, and Yimei Zhu

Abstract

There is a wide array of technologically significant materials whose response to electric and magnetic fields can make or break their utility for specific applications. Often, these electrical and magnetic properties are determined by nanoscale features that can be most effectively understood through electron microscopy studies. Here, we present an overview of the capabilities for transmission electron microscopy for uncovering information about electric and magnetic properties of materials in the context of operational devices. When devices are operated during microscope observations, a wealth of information is available about dynamics, including metastable and transitional states. Additionally, because the imaging beam is electrically charged, it can directly capture information about the electric and magnetic fields in and around devices of interest. This is perhaps most relevant to the growing areas of nanomaterials and nanodevice research. Several specific examples are presented of materials systems that have been explored with these techniques. We also provide a view of the future directions for research.

Introduction

In the development of the light microscope as an instrument of science and technology, much of the credit goes not to the Dutch who invented the device, or Hooke and others, who were among the first to use the tool for scientific research, but rather to Antoni van Leeuwenhoek, who was the first to put living organisms behind its lens.[1] In this sense, Leeuwenhoek was the first to practice *in situ* microscopy in his research and thus establish the microscope as a tool for uncovering the origins and inner workings of life itself. Today, the electron microscope is proving itself a valuable tool in uncovering the inner workings of electronic devices in a similar way. A large part of the value of *in situ* investigations is the ability of an electron microscope to provide a "live" image of a device under study. In this way, any changes to the structure or properties of the device can be recorded and noted as they occur. Thus, it is straightforward to capture intermediate or metastable states of devices during operation or, sometimes more importantly, during failure. Of equal importance is the fact that electron microscopes utilize electrons as a characterization probe, which enables unique information to be gathered about the electric and magnetic fields in and around a device, by virtue of the electric charge carried by the electrons.

This review is not meant to be an exhaustive look at the study of electric and magnetic fields in samples. Rather, our mission is to give an overview of the types of studies that have been done and to give a feel for where we as authors see the field going. We first give an overview of the methods of transmission electron microscopy (TEM) for gathering this electromagnetic information, followed by an overview of the specific application of these techniques to the study of magnetic materials and structures. We then move on to an overview of electric devices that have been studied by TEM. Last, we introduce a growing area of work where direct nanoscale manipulation is used to create and study devices *in situ* during observations. Finally, we give an outlook toward the future of *in situ* TEM studies of electric and magnetic devices.

Methods of Obtaining Electric and Magnetic Information
Instrumentation

For *in situ* microscopy studies, a specialized specimen holder is often needed to introduce fields or electrical connections in the restricted specimen space that most TEMs afford. Various holders have been developed in recent years for measuring electrostatic and magnetostatic potentials, such as *p–n* junctions of a semiconductor device[2] and switching behavior of patterned magnetic elements.[3] Some examples of customized specimen holders are shown in Figure 1. Sometimes a dedicated instrument might be required for studying magnetic phenomena. The key experimental hurdle to magnetic imaging is to reduce the normally strong magnetic field at the specimen (typically about 20 kOe) down to a level that does not perturb the magnetic structure of the sample, sometimes referred to as a Lorentz imaging condition. Although in modern electron microscopes the objective lens can easily be turned off and the pre-field objective lens used for focusing, the remanent field in the sample area in this mode is still too large (200–300 Oe) for most soft magnetic materials. There are a few dedicated instruments worldwide that are designed for magnetic imaging and holography.[4] This is typically achieved either by turning off the standard objective lens and focusing using a weaker "Lorentz" lens below the sample (sometimes with an extra condenser lens above the sample to further cancel residual fields) or by using a dedicated Lorentz objective lens.[5] The second option uses a weakly-excited long
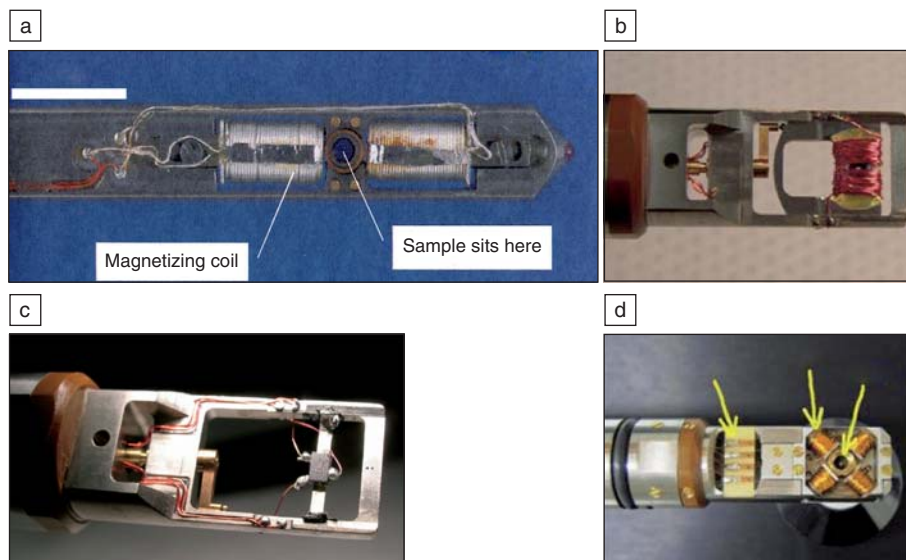
Figure 1. Various magnetic-measurement specimen holders for TEM. (a, b) Custom-built holders for applying uniaxial magnetic fields. Holders by (a) Oxford University and (b) Brookhaven National Lab. (c) Home-made Hall-probe to calibrate the magnetic field in the sample area. Holder by Brookhaven National Lab. (d) Custom-made two-axis magnetic holder with rotation capabilities by Gatan-UK.
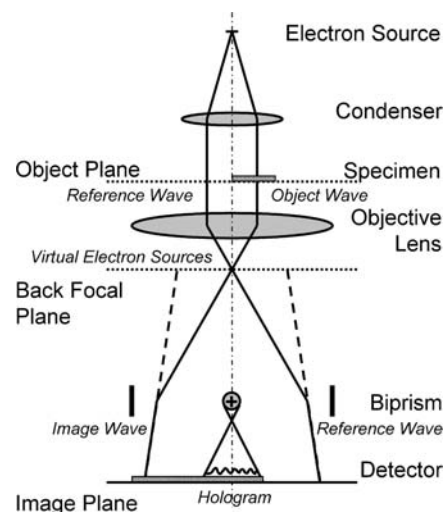

Figure 2. A schematic diagram of off-axis electron holography. In this technique, an image wave that travels through the specimen is allowed to overlap with a reference wave that does not. The resulting interference fringes carry information about the electric and magnetic potentials in the specimen (from Reference 6).

focal length objective (with a focal length on the order of 17 mm as opposed to ~2 mm for a standard lens) with the specimen located above the pole-piece gap, so that the magnetic field at the sample area is significantly reduced to only a few Oersted with the lens activated (3–4 orders of magnitude smaller than a standard objective lens). The aberration coefficients of a dedicated Lorentz objective lens are about two orders of magnitude smaller than that measured for the other configurations, resulting in much better resolution. To produce high-performance electron holography data certain requirements must be met—as an example, the 2100F-LM instrument at Brookhaven National Laboratory[5] provides about 17% of fringe contrast in the sample for a hologram with 1.5 nm fringe spacing (see *electron holography*, below). This gives ~5–6 nm point resolution in the reconstructed phase with a phase sensitivity of $\pi/40$.

Methods

As in neutron and x-ray scattering studies, electron microscopy detectors can only record the intensity (amplitude-squared) of the wave function of the transmitted electron beam. However, the imaging electrons can be treated as waves, and as such they carry both amplitude and phase. Furthermore, as electrons travel through electric and magnetic fields, their phase is modified. Thus, recovering the phase of the electron wave is the key to obtaining the electric and magnetic information of the sample. Two techniques, electron holography and Lorentz microscopy, are commonly used for this purpose.

1. Electron holography, in its most widely used form, is based on the interference between an electron wave that goes through the specimen (the object wave), and a reference wave that does not.[6] The information in the object wave is first recorded as an interference pattern, or electron hologram, by superimposing the object wave with the reference wave. A schematic of this is shown in Figure 2. From this, the phase is then reconstructed digitally using Fourier analysis. Off-axis electron holography is the most straightforward approach, where the reference wave, usually acquired from a vacuum region near the area of interest, is somewhat tilted relative to the object wave. The two waves are brought into interference in an intermediate image plane by means of an electrostatic biprism. The resulting fringe pattern is then recorded on a charge-coupled device (CCD) camera as a hologram. The hologram is first Fourier-transformed to obtain the corresponding power spectrum, which contains an autocorrelation component and two sideband components that carry the desired phase information about the object. One of these first-order sidebands is selected for reconstruction, and a digital filter can be employed to correct aberrations. The filtered sideband is then inverse Fourier-transformed to obtain the complex object wave function, which can be displayed as an amplitude or phase image of the object. Electron holography thus offers the unique capabilities to recover the phase shift of an electron wave and to retrieve the electrostatic and magnetostatic potentials associated with the sample. To determine these potentials one must examine the quantum mechanical phase that the electrons accumulate in traveling through the potentials, and a detailed description of this is given in Reference 6. The key figures of merit that determine the usefulness of holography are the fringe contrast and fringe spacing. Fringe contrast is determined by the level of coherence of the electron source, and is only at a useful level (tens of percents) for a field-emission source. Fringe spacing ultimately determines the spatial resolution of the technique.

2. Lorentz microscopy is a classical imaging method for observing magnetic domains. It is also based on phase contrast (i.e., the phase shift of the incident beam caused by the magnetic vector potential and the enclosed magnetic flux). Two imaging modes are routinely used, shown schematically in Figure 3. One is the Fresnel mode, where the image contrast is formed by under- or over-focusing of the sample. The Fresnel contrast, appearing at the locations where the potentials alter, increases with defocus value. The other
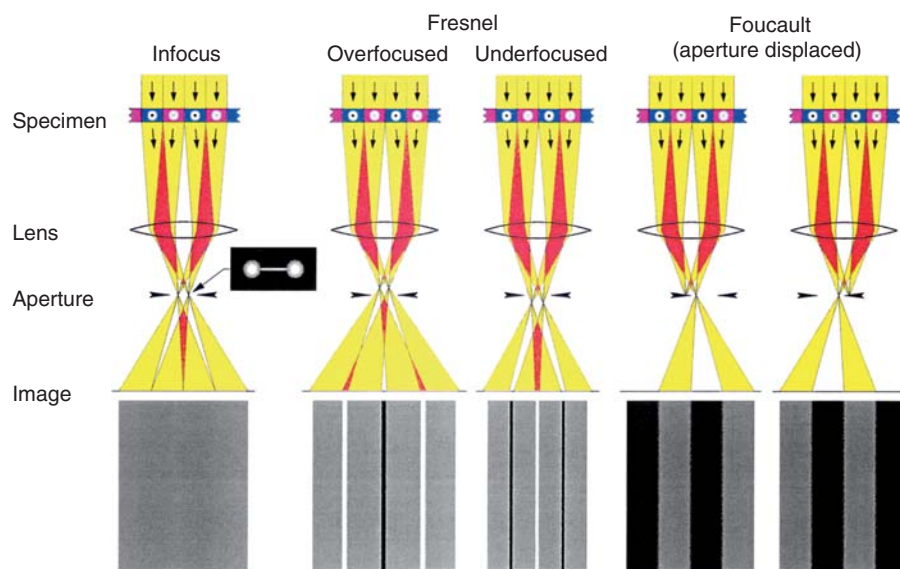
Figure 3. A schematic diagram of the Fresnel and Foucault modes of Lorentz microscopy (from Reference 67).

is the Foucault mode. In the Foucault mode, the sample is imaged in-focus. To form a magnetization-direction-sensitive Foucault image, a small aperture is used to select the slightly deflected electrons in the back-focal plane (deflection angles are usually 10^3 times smaller than the Bragg angles) due to the magnetic structure (or Lorentz force) in the sample, similar to dark-field imaging in conventional TEM. Thus, Fresnel mode is used to image the domain-wall position, whereas the Foucault mode is used to image the domains. Fresnel mode is not limited to observing magnetic structure, as it is also sensitive to changes of electrostatic potential in the sample.

Recently, significant efforts have been made to use Fresnel images to retrieve the phase of the wave function based on the transport-of-intensity equation (TIE) to map local magnetization. TIE relates the phase of an image wave to its recorded intensity.[7] It requires two or more Fresnel images at different defocus for phase retrieval. In comparison with electron holography, the TIE method does not require special hardware and has a larger area of view. Mathematically, the equation is not difficult to solve. However, in practice, it can be quite a challenging task, and the result often suffers from image artifacts. The quality of the phase retrieval largely depends on the property of the images, imaging parameters (especially the defocus value), the alignment of the images, and the correction of the rotation and optical distortion of the images.[8]

Extreme care must be taken in interpreting the recovered phase images.

As both electric and magnetic information are encoded in the phase of the wave function, it is essential to separate the two to understand the behavior of the materials (local thickness variation of the sample directly relates to a change of projected electrostatic potential). To distinguish the two sets of information, one can flip the sample upside-down and sum the image intensities of the same sample areas. Whereas magnetic structures can show a contrast reversal during a 180° flip of the sample, structures related to electrostatic potential do not. Because images are recorded in projection in TEM, the mapping of magnetic or ferroelectric domain structures also depends on the particular orientation of the domains.

Imaging Magnetic Fields—Domain Dynamics and Magnetization Reversal Processes

TEM has been widely used to study magnetic films and nanostructures, and inevitably a review of this scope will only include a small subset of the range of materials systems that have been studied. *In situ* magnetic fields can be applied to a sample while imaging in the TEM, which enables the *local* magnetization reversal of a sample to be followed in real time, in addition to imaging the remanent state of a magnetic nanostructure. For example, Lau et al. showed that the remanent magnetic state of arrays of micron-sized

Permalloy ($Ni_{80}Fe_{20}$) thin film elements is a function of the rate of change of the applied field, with low rates giving a multidomain state and fast reversal favoring a single vortex state.[9,10] At present, limitations on image capture and signal mean that the shortest time interval that can be achieved is typically 16–40 ms, although efforts are being made to reduce this further. With this time resolution it is essentially the quasi-static behavior of the magnetization that is being analyzed, rather than the true dynamics, for which the time resolution required is on the order of nanoseconds or even picoseconds. However, the existing time resolution can provide a wealth of information about the behavior of magnetic thin films and nanostructures.

For example, electron holography studies of the magnetic reversal behavior in nanoscale circular Co rings has shown that cutting slots into the rings decreases the field range over which reversal occurs and results in a more uniform reversal mechanism.[11] Structures of this type are being considered for potential applications in information storage, so understanding the details of their response to a magnetic field is of considerable technological relevance. The motion of domain walls through magnetic nanostructures is also being investigated as a means of producing magnetic logic circuits, and Lorentz TEM has shown how constrictions in nanoscale Permalloy elements can act as domain wall traps, controlling not only the motion of the walls, but also the specific domain wall configuration.[12] Analyzing the magnetic behavior of elongated structures such as magnetic nanopillars presents a challenge to TEM studies because the technique is only sensitive to the magnetic induction normal to the electron beam. By cutting out single rows of Ni nanopillars from arrays and mounting them with their long axis perpendicular to the electron beam, the reversal mechanism and interactions between pillars were shown to depend strongly on the microstructure, which could also be analyzed in the TEM.[13] Figure 4 shows two phase images of Ni pillars (175 nm tall, 75 nm diameter) reconstructed from electron holography images. The images show the remnant states of the pillars after application of *in situ* magnetic fields of the magnitude indicated in the images. The color wheel indicates the direction of magnetization in the pillars, and the effect of the grain structure can be seen from the variations in magnetization direction within each pillar.

The ability to carry out Lorentz TEM within a range of temperatures has been
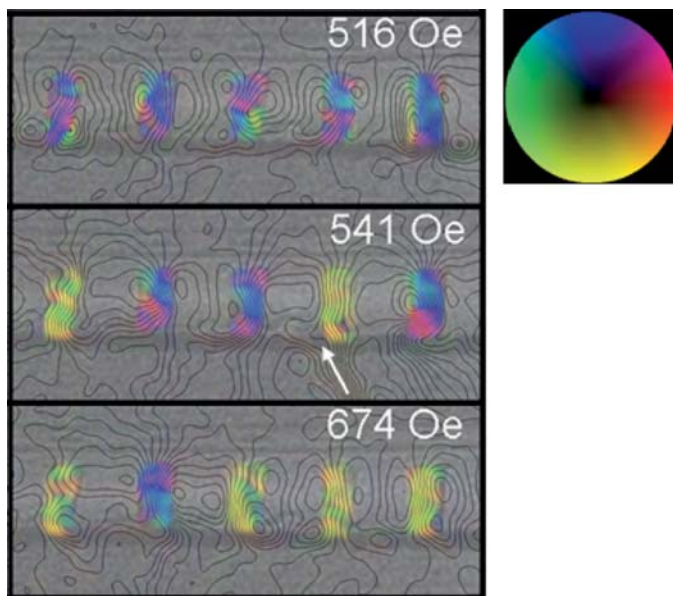
Figure 4. Phase images showing magnetic induction in Ni nanopillars (175 nm high, 75 nm diameter) at remanance after *in situ* application of field value indicated. The color wheel indicates the direction of the magnetic induction. Note also the flux lines between pillars, which show how the interaction between adjacent pillars varies depending on their relative direction of magnetization.

put to very good effect by Togawa and co-workers to study the behavior of the vortex lattice in thin films of superconductors.[14] Movies showing the motion of vortices at induced defects in Nb show very clearly the way in which the vortices interact with each other, for example by annihilation, and with the defects. The technique was also used successfully to elucidate the structure of chain vortices in $YBaCu_3O_{7,8}$ (YBCO) and $Bi_2Sr_2CaCu_2O_{8+\delta}$.[15]

Wiring it Up: *In Situ* Devices

There is great promise for exploring the world of electronic and magnetic devices by looking at active functional devices *in situ*. This promise has been apparent since early studies looked at operational scanning tunneling devices and semiconductor devices in the early 1990s.[16–18] However, there are a number of challenges to performing *in situ* TEM studies of devices, and there remains a great potential for future exploration. The foremost of these challenges is the requirement for electron transparency. To be amenable to TEM imaging, materials can range in thickness from tens of nanometers up to a few hundred nanometers. Most devices do not fall in this range, and typically one must fabricate a specialized version of a device concept for *in situ* TEM studies. However, vacuum devices, such

as field emission devices, are naturally amenable to study, as are devices fabricated on the nanoscale using nanotubes and nanowires. One of the more impressive devices that has been observed with *in situ* TEM is a fully functioning electrochemical cell fabricated for the purpose of studying the nucleation and growth of electrodeposited films.[19–21] The electrochemical cell, operating sealed in vacuum as an electron-transparent structure, has opened doors for new material systems that can be studied as *in situ* devices.

The combination of electron holography and *in situ* devices has been used to study the electric fields present in biased and unbiased semiconductor *p-n* junctions.[22–27] These results have revealed, among other results, that there can be an electrostatic "dead layer" in these devices near their surfaces. Electron holography has also been used to study charged microtips[28] and field-emission from carbon nanotubes.[29] In the latter case, the electric field was shown to be stable even though the emission current through the device may fluctuate. As a further example, Lorentz TEM has been successfully used to complete *in situ* magnetotransport studies of active devices. For example, by recording images of the magnetization reversal simultaneously with measurement of the giant magnetoresistance, the magnetotransport behavior of a litho-

graphically patterned $NiFe_{8nm}/Cu_{3nm}/Co_{2nm}/NiFe_{6nm}/NiMn_{25nm}$ spin valve could be directly analyzed. For these experiments the specimen was connected via Au contacts to an external circuit so that a current could be passed through the specimen *in situ* in the TEM while magnetizing.[30] More recently, a similar technique was used to image the domain wall motion as a result of the spin-torque effect in nanoscale zig-zag Permalloy wires.[31] A current was used to excite the wall motion, and a series of careful experiments distinguished the effects of thermal excitation and spin-torque.

Part of the appeal of looking at active electric and magnetic devices with TEM is the ability to characterize the structure of the device down to the atomic level using high-resolution imaging. In no area is this more applicable than in the case of devices where the active region only has atomic dimensions. This is the case in a scanning tunneling microscope (STM)[16,32–34] and also in atomic-scale metal wires.[35] Studies on such devices have revealed the crossover from ballistic sizes (where the size is too small to support sufficient scattering) to standard diffusive transport.[36] Additionally, electrical conduction through a single chain of gold atoms has also been reported.[35] In these studies, the junction is created mechanically by pulling apart narrow contacts (see also the next section, "Nanomanipulation-Making Devices *In Situ*"). However, another study explores the possibility of creating these contacts electrically by taking advantage of electromigration to thin small junctions of atomic-scale dimensions.[37]

One material that has received particularly intense study as an electrically active device material has been carbon nanotubes. Early *in situ* studies examined the electrical properties of nanotubes contacted by liquid metals.[38–40] In addition to the field-emission studies referred to above, they have been explored for mechanical devices, such as rotational elements,[41–46] bearings,[41,47,48] and variable resistors.[49] In these, they have shown interesting electromechanical properties owing to the ability of the concentric nanotube layers to slide past one another. Electrically actuated mechanical resonance studies have also shown similarly peculiar interlayer mechanics.[50]

Nanomanipulation—Making Devices *In Situ*

The design and fabrication of nanoscale devices are challenging because of the small dimensions. It becomes increasingly difficult to both see and manipulate the small parts and structures as the sizes

approach atomic dimensions. The introduction of scanning probe microscopes in the TEM has opened new opportunities on the nanometer and subnanometer scale by enabling simultaneous imaging and manipulation/spectroscopy with high spatial resolution and precision. An important aspect is that the dynamics of the processes can be observed.

Most manipulators are based on regular side-entry TEM holders that are modified to contain a piezotube that allows a manipulator to be moved in *x*-, *y*-, and *z*-directions.[34,35,50–53] An example of such a holder is shown in Figure 5. There are also examples where a MEMS electrostatic actuator is used to achieved the motion.[54] The function of the manipulator can be a nanoindentor or an STM, but it also enables *in situ* manipulation of structures on the nanoscale. Examples of nanodevices that have been made and illustrated using *in situ* manipulation are linear nanobearings,[47,48] variable resistors,[49] tunable nanoresonators,[53] nanoscale rotational actuators,[41] mass conveyors,[55] metal nanopipettes,[56] nanobalances,[50] switches,[57] oscillators,[58] and field emitters.[29,59] Very often nanowires and tubes are used as the main component of the nanodevice.

There is a twofold benefit from using the TEM for *in situ* manipulation. The first is the direct observation of the structures that are being made. The second is the ability to directly correlate the structures to properties and provide information that reveals the basic mechanisms that enable the realization of new nanodevices with unique and tailored properties. The processes of electromigration,[55,56] telescoping of carbon nanotubes,[47,48,53] field emission,[29,59] and electromechanical resonances[50,53,58] have been studied and used to make nanodevices.

Experiments on carbon nanotubes filled with metals[56,60] or with metal particles on the outer surface[55] have shown that electromigration can be used to convey and deposit small masses. The mass transport rate depends on the applied electric field, and the direction of the migration is determined by the polarity. It is interesting to note that the electromigration wind force is prevailing for iron-[56] and cobalt-filled[60] carbon nanotubes whereas the direct forces appear to be predominant for indium particles on the surface.[55] The migration of metal within the carbon nanotubes can be used for a pipette function to deposit small particles with high precision to build three-dimensional structures, and here there is a threshold current density for the onset of electromigration.[56] It can also be used for zone refinement or growth of
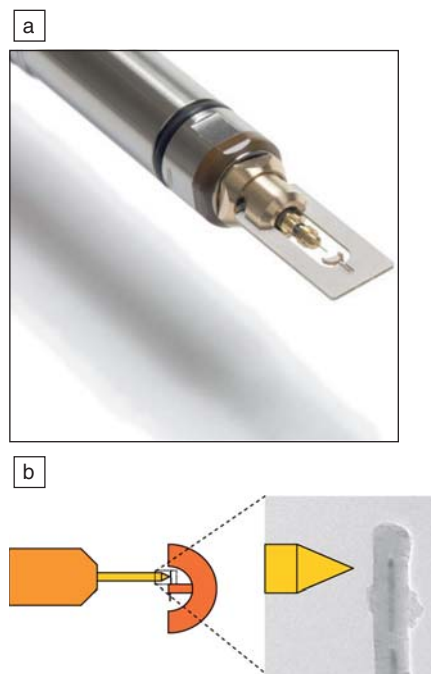
Figure 5. (a) A transmission electron microscopy-scanning tunneling microscopy manipulation holder, manufactured by Nanofactory Instruments.[34] The holder enables both coarse and fine motion of the STM tip in *x*-, *y*-, and *z*-direction. (b) A schematic illustrating the tip and the sample.

higher crystal quality tubes where the metal filling acts as a catalyst for the carbon nanotube growth.[60] Carbon nanotubes without filling or particles on the surface can be reshaped by electromigration and high temperature annealing, enabling control of the diameter of the tube.[61,62]

Carbon nanotubes are recognized as potential components of nanoscopic systems. Toward this end, they are frequently used in nanomanipulation experiments making small electromechanical devices. One possible application is a nanobalance for nanoparticles.[50] A carbon nanotube that is attached at one end and exposed to an oscillating voltage at the free tip (but without direct contact) can start to vibrate. The nanotube bends because it becomes electrically charged under the influence of the voltage and the charge is located at the tip of the nanotube. The force exerted by the voltage causes a bending of the tube. The resonance frequency depends on the length, the elastic modulus, and the inner and outer diameters of the carbon nanotube. A mass attached to the tip of the nanotube alters the resonance frequency, providing the nanobalance function. Masses on the order of 10^{-15} g can be deter-

mined. The same principle of resonant frequencies can be used for a carbon nanotube attached at both ends giving a nanoresonator where the resonance frequency can be tuned using a telescopic effect of a multiwalled nanotube.[53]

TEM *in situ* manipulators provide a surgical tool to reach into the nano- and atomic world of materials and devices. Dynamic processes can be observed, and the direct live information about the interplay between structure and properties enables precise control of nanostructures. New methods to reproducibly fabricate nanodevices can be developed; in addition it is possible to obtain a direct fundamental understanding of the importance of individual interfaces and defects for the properties.

Conclusion and Look to the Future

From this review, we hope that the reader is able to get a feel for the capabilities of TEM to uncover electric and magnetic phenomena through *in situ* studies. A lot of progress has been made, and a capable set of tools are available, but the field is still very much in its infancy. For instance, the dimensions of TEM samples were standardized long ago to 3 mm discs, but there is still no accepted standard for samples with electrical contacts. For electrical measurements, different research groups must develop their own contact configuration and measurement platforms. Whereas several vendors will manufacture custom electrical measurement specimen holders (e.g., Gatan, Fischione, Nanofactory Instruments, Hummingbird Scientific), there has yet to emerge a common platform for multiple electrical contacts to specimens.

As far as future research directions, the authors see a huge potential for uncovering new phenomena with the techniques described herein. For example, one of us is currently performing *in situ* studies of the transport properties of electrically-biased magnetic tunnel junctions.[63] Here, the capability to directly observe the region of tunneling with Lorentz and high-resolution microscopy should allow an unprecedented level of characterization of these common devices. Another of us has recently demonstrated a new technique for electron thermal microscopy of active devices.[64] The technique has the power to image non-uniform temperature distributions in active nanowire and nanotube electronics. Additionally, there is great promise for studying the active evolution of the magnetic state of rationally-designed nanomagnetic lattices, such as the recently invented artificial spin ice.[65] These model magnetic structures may

answer long-standing questions about the third law of thermodynamics in the context of proton disorder in crystalline ice. Atomic resolution and nanoscale manipulation studies also stand poised to resolve some of the mysteries of vacuum tunneling, as the ability to visualize the tunnel junction directly is a powerful ability not typically afforded by the common scanning tunneling geometry. We also see great promise in being able to explore the growing area of current-induced domain wall motion in magnetic nanowires. Here, the capabilities of Lorentz microscopy for real-time imaging of domain wall structures should enable a comprehensive exploration of the parameters involved in this phenomenon. Finally, the prospects for exploring the response of materials under electric stimulus, such as the current-induced motion of vortices in superconductors and polarons in manganites with colossal magnetoresistance effects,[66] can shed light on our understanding of the underlying mechanisms of intriguing properties, thus clearing the way for increased application of these materials. Clearly, there is a wealth of opportunities for new research, and the future will light the way.

References

1. B.J. Ford, *The Leeuwenhoek Legacy* (Biopress Ltd., Bristol, 1991).
2. D. Cooper, A.C. Twitchett-Harrison, P.A. Midgley, R.E. Dunin-Borkowski, *J. Appl. Phys.* **101**, 094508 (2007).
3. J.W. Lau, M.A. Schofield, Y. Zhu, *Ultramicroscopy* **107**, 396 (2007).
4. Y. Murakami, D. Shindo, *Mater. Trans.* **46**, 743 (2005).
5. M.A. Schofield, M. Beleggia, J. W. Lau, and Y. Zhu, *JEOL News,* 2 (2007).
6. M. Lehmann, H. Lichte, *Microsc. Microanal.* **8**, 447 (2002).
7. K.A. Nugent, T.E. Gureyev, D.F. Cookson, D. Paganin, Z. Barnea, *Phys. Rev. Lett.* **77**, 2961 (1996).
8. M. Beleggia, M.A. Schofield, V.V. Volkov, Y. Zhu, *Ultramicroscopy* **102**, 37 (2004).
9. J.W. Lau, M. Beleggia, M.A. Schofield, G.F. Neumark, Y. Zhu, *J. Appl. Phys.* **97**, 10E702 (2005).
10. J.W. Lau, M. Beleggia, Y. Zhu, *J. Appl. Phys.* **102**, 043906 (2007).
11. H. Hu, H. Wang, M.R. McCartney, D.J. Smith, *Phys. Rev. B.* **73**, 153401 (2006).
12. C. Brownlie, S. McVitie, J.N. Chapman, C.D.W. Wilkinson, *J. Appl. Phys.* **100**, 033902 (2006).
13. T.J. Bromwich, T. Kasama, R.K.K. Chong, R.E. Dunin-Borkowski, A.K. Petford-Long, O.G. Heinonen, C.A. Ross, *Nanotechnology* **17**, 4367 (2006).

14. Y. Togawa, K. Harada, T. Akashi, H. Kasai, T. Matsuda, A. Maeda, A. Tonomura, *Physica C* **426**, 141 (2005).
15. A. Tonomura, H. Kasai, O. Kamimura, T. Matsuda, K. Harada, T. Yoshida, T. Akashi, J. Shimoyama, K. Kishio, T. Hanaguri, K. Kitazawa, T. Masui, S. Tajima, N. Koshizuka, P.L. Gammel, D. Bishop, M. Sasase, S. Okayasu, *Phys. Rev. Lett.* **88**, 237001 (2002).
16. J.C.H. Spence, W. Lo, M. Kuwabara, *Ultramicroscopy* **33**, 69 (1990).
17. F.M. Ross, R. Hull, D. Bahnck, J.C. Bean, L.J. Peticolas, R.A. Hamm, H.A. Huggins, *J. Vac. Sci. Technol. B* **10**, 2008 (1992).
18. F.M. Ross, R. Hull, D. Bahnck, J.C. Bean, L.J. Peticolas, C.A. King, *Appl. Phys. Lett.* **62**, 1426 (1993).
19. M.J. Williamson, R.M. Tromp, P.M. Vereecken, R. Hull, F.M. Ross, *Nat. Mater.* **2**, 532 (2003).
20. A. Radisic, P.M. Vereecken, P.C. Searson, F.M. Ross, *Surf. Sci.* **600**, 1817 (2006).
21. A. Radisic, F.M. Ross, P.C. Searson, *J. Phys. Chem. B* **110**, 7862 (2006).
22. A. Lenk, H. Lichte, U. Muehle, *J. Electron. Microsc.* **54**, 351 (2005).
23. S. Frabboni, G. Matteucci, G. Pozzi, M. Vanzi, *Phys. Rev. Lett.* **55**, 2196 (1985).
24. W.D. Rau, P. Schwander, A. Ourmazd, *Phys. Status Solidi B* **222**, 213 (2000).
25. W.D. Rau, P. Schwander, F.H. Baumann, W. Hoppner, A. Ourmazd, *Phys. Rev. Lett.* **82**, 2614 (1999).
26. A.C. Twitchett, R.E. Dunin-Borkowski, P.A. Midgley, *Phys. Rev. Lett.* **88**, 238302 (2002).
27. A.C. Twitchett, R.E. Dunin-Borkowski, R.F. Broom, P.A. Midgley, *J. Phys.: Condens. Matter* **16**, S181 (2004).
28. G. Matteucci, G.F. Missiroli, M. Muccini, G. Pozzi, *Ultramicroscopy* **45**, 77 (1992).
29. J. Cumings, A. Zettl, M.R. McCartney, J.C.H. Spence, *Phys. Rev. Lett.* **88**, 056804 (2002).
30. X. Portier, E.Y. Tsymbal, A.K. Petford-Long, T.C. Anthony, J.A. Brug, *Phys. Rev. B.* **58**, R591 (1998).
31. F. Junginger, M. Kläui, D. Backes, U. Rüdiger, T. Kasama, R.E. Dunin-Borkowski, L.J. Heyderman, C.A.F. Vaz, J.A.C. Bland, *Appl. Phys. Lett.* **90**, 132506 (2007).
32. Y. Naitoh, K. Takayanagi, M. Tomitori, *Surf. Sci.* **358**, 208 (1996).
33. J. Yamashita, H. Hirayama, Y. Ohshima, K. Takayanagi, *Appl. Phys. Lett.* **74**, 2450 (1999).
34. K. Svensson, Y. Jompol, H. Olin, E. Olsson, *Rev. Sci. Instrum.* **74**, 4945 (2003).
35. H. Ohnishi, Y. Kondo, K. Takayanagi, *Nature* **395**, 780 (1998).
36. D. Erts, H. Olin, L. Ryen, E. Olsson, A. Tholen, *Phys. Rev. B.* **61**, 12725 (2000).
37. D.R. Strachan, D.E. Smith, M.D. Fischbein, D.E. Johnston, B.S. Guiton, M. Drndic, D.A. Bonnell, A.T. Johnson, *Nano Lett.* **6**, 441 (2006).
38. Z.L. Wang, P. Poncharal, W.A. de Heer, *Pure Appl. Chem.* **72**, 209 (2000).
39. Z.L. Wang, P. Poncharal, W.A. de Heer, *J. Phys. Chem. Solids* **61**, 1025 (2000).
40. Z.L. Wang, P. Poncharal, W.A. de Heer, *Microsc. Microanal.* **6**, 224 (2000).

41. A.M. Fennimore, T.D. Yuzvinsky, W.Q. Han, M.S. Fuhrer, J. Cumings, A. Zettl, *Nature* **424**, 408 (2003).
42. S.J. Papadakis, A.R. Hall, P.A. Williams, L. Vicci, M.R. Falvo, R. Superfine, S. Washburn, *Phys. Rev. Lett.* **93**, 146101 (2004).
43. P.A. Williams, S.J. Papadakis, A.M. Patel, M.R. Falvo, S. Washburn, R. Superfine, *Phys. Rev. Lett.* **89**, 255502 (2002).
44. P.A. Williams, S.J. Papadakis, A.M. Patel, M.R. Falvo, S. Washburn, R. Superfine, *Appl. Phys. Lett.* **82**, 805 (2003).
45. J.C. Meyer, M. Paillet, S. Roth, *Science* **309**, 1539 (2005).
46. J.C. Meyer, J. Cech, B. Hornbostel, S. Roth, *Phys. Status Solidi B* **243**, 3500 (2006).
47. J. Cumings, P. G. Collins, A. Zettl, *Nature* **406**, 586 (2000).
48. J. Cumings, A. Zettl, *Science* **289**, 602 (2000).
49. J. Cumings, A. Zettl, *Phys. Rev. Lett.* **93**, 086801 (2004).
50. P. Poncharal, Z.L. Wang, D. Ugarte, W.A. de Heer, *Science* **283**, 1513 (1999).
51. T. Kizuka, K. Yamada, S. Deguchi, M. Naruse, N. Tanaka, *Phys. Rev. B.* **55**, R7398 (1997).
52. A.M. Minor, J.W. Morris, E.A. Stach, *Appl. Phys. Lett.* **79**, 1625 (2001).
53. K. Jensen, Ç. Girit, W. Mickelson, A. Zettl, *Phys. Rev. Lett.* **96**, 215503 (2006).
54. M.I. Lutwyche, Y. Wada, *Appl. Phys. Lett.* **66**, 2807 (1995).
55. B.C. Regan, S. Aloni, R.O. Ritchie, U. Dahmen, A. Zettl, *Nature* **428**, 924 (2004).
56. K. Svensson, H. Olin, E. Olsson, *Phys. Rev. Lett.* **93**, 145901 (2004).
57. K.J. Ziegler, D.M. Lyons, J.D. Holmes, D. Erts, B. Polyakov, H. Olin, K. Svensson, E. Olsson, *Appl. Phys. Lett.* **84**, 4074 (2004).
58. B.C. Regan, S. Aloni, K. Jensen, A. Zettl, *Appl. Phys. Lett.* **86**, 123119 (2005).
59. M. Sveningsson, K. Hansen, K. Svensson, E. Olsson, E.E.B. Campbell, *Phys. Rev. B.* **72**, 85429 (2005).
60. K. Jensen, W. Mickelson, W. Han, A. Zettl, *Appl. Phys. Lett.* **86**, 173107 (2005).
61. T.D. Yuzvinsky, W. Mickelson, S. Aloni, G.E. Begtrup, A. Kis, A. Zettl, *Nano Lett.* **6**, 2718 (2006).
62. A. Koshio, M. Yudasaka, S. Iijima, *J. Phys. Chem. C* **111**, 10 (2007).
63. A.N. Chiaramonti, D.K. Schreiber, B. Kabius, W.F. Egelhoff, A.K. Petford-Long, *Microsc. Microanal.* **13**, 626CD (2007).
64. T. Brintlinger, Y. Qi, K.H. Baloch, D. Goldhaber-Gordon, J. Cumings, *arxiv.org/archive/cond-mat* (2007); arXiv:0708.1522.
65. R.F. Wang, C. Nisoli, R.S. Freitas, J. Li, W. McConville, B.J. Cooley, M.S. Lund, N. Samarth, C. Leighton, V.H. Crespi, P. Schiffer, *Nature* **439**, 303 (2006).
66. C. Jooss, L. Wu, T. Beetz, R.F. Klie, M. Beleggia, M.A. Schofield, S. Schramm, J. Hoffman, Y. Zhu, *Proc. Natl. Acad. Sci.* **104**, 13597 (2007).
67. A.K. Petford-Long, J.N. Chapman, in *Magnetic Microscopy of Nanostructures* **4**, H. Hopster, H.P. Oepen, Eds., (Springer, Berlin, 2005).